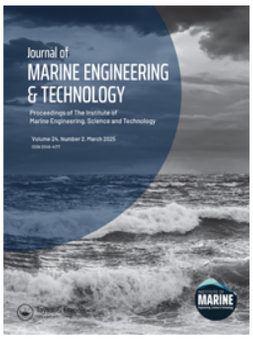

Journal of Marine Engineering & Technology

ISSN: 2046-4177 (Print) 2056-8487 (Online) Journal homepage: www.tandfonline.com/journals/tmar20

The assessment of alternative fuel and engine power limitation utilisation in hybrid marine propulsion systems regarding energy efficiency metrics

Onur Yuksel, Murat Pamik & Murat Bayraktar

To cite this article: Onur Yuksel, Murat Pamik & Murat Bayraktar (18 Mar 2025): The assessment of alternative fuel and engine power limitation utilisation in hybrid marine propulsion systems regarding energy efficiency metrics, Journal of Marine Engineering & Technology, DOI: 10.1080/20464177.2025.2479319

To link to this article: https://doi.org/10.1080/20464177.2025.2479319

Published online: 18 Mar 2025.

JOURNAL OF MARINE ENGINEERING & TECHNOLOGY
https://doi.org/10.1080/20464177.2025.2479319

Taylor & Francis
Taylor & Francis Group

The assessment of alternative fuel and engine power limitation utilisation in hybrid marine propulsion systems regarding energy efficiency metrics

Onur Yuksel [a,b], Murat Pamik [c] and Murat Bayraktar [b]

[a]Liverpool Logistics Offshore and Marine Research Institute (LOOM), Faculty of Engineering, Liverpool John Moores University, Liverpool, UK; [b]Zonguldak Bülent Ecevit University, Marine Engineering, Maritime Faculty, Kdz. Ereğli/Zonguldak, Türkiye; [c]Dokuz Eylül University, Marine Engineering, Maritime Faculty, Buca/İzmir, Türkiye

ABSTRACT

The adoption of alternative fuels is vital for meeting maritime decarbonisation targets. While various options exist, liquefied natural gas (LNG) is the leading choice, with methanol gaining ground. Integrating LNG and methanol in hybrid propulsion systems (HPSs) improves operational efficiency and ensures compliance with energy efficiency standards. This study explores the environmental benefits of HPSs using a scenario-based approach in which the existing propulsion system of a Ro-Ro (Roll-on/Roll-off) cargo ship is replaced with HPSs powered by LNG, methanol, or conventional fuels. Results demonstrate that implementing HPS alone on the vessel reduces fuel consumption by up to 21% across all scenarios by managing power fluctuations in the main engines. The LNG-HPS scenario lowers the attained Carbon Intensity Indicator (CII) by 36% to 4.13, keeping the CII rating at level A until the end of 2026. The methanol-HPS scenario achieves a fuel reduction of up to 22%, yet none of the scenarios meets the Energy Efficiency Design Index (EEDI) Phase III threshold of 7.65. To surpass this threshold, vessel speed reduction applications with alternative fuel utilisation, are evaluated. This integration improves the case ship's EEDI to 6.2 for LNG and 7.3 for methanol scenarios, exceeding threshold values for energy efficiency metrics.

ARTICLE HISTORY
Received 21 July 2024
Accepted 10 March 2025

KEYWORDS
Alternative fuels; hybrid power system (HPS); Energy Efficiency Design Index (EEDI); Energy Efficiency Existing Ship Index (EEXI); Carbon Intensity Indicator (CII)

List of abbreviations

B_s	Breadth
C_F	Carbon Factor
C_{FAE}	C_F of the Fuel Used for Auxiliary Engine
C_{FME}	C_F of the Fuel Used for Main Engines
CII	Carbon Intensity Indicator
DF	Dual fuel
d_s	Summer load line draught
DWT	Deadweight tonnage
EEDI	Energy Efficiency Design Index
EEXI	Energy Efficiency Existing Ship Index
EPL	Engine Power Limitation
F_{n_L}	Froude number
f_c	Correction Factor for Ships with Alternative Cargo Types Showing the DWT-Capacity Relationship
f_{eff}	Correction Factor Used If Technologies Are Available
f_i	Capacity correction factor for ice-class ships
f_j	Correction Factor for Ships with Special Design Features
f_l	Factor for general cargo ships equipped with cranes and other cargo-related gear
f_m	Factor for ice-classed ships capable of navigating challenging ice conditions with icebreaker assistance.
f_w	The factor of speed decrease at sea
g	Gravitational acceleration
HPS	Hybrid propulsion system
IMO	International Maritime Organisation
LCV	Lower calorific value
LNG	Liquefied Natural Gas
L_{pp}	Length between perpendiculars
MCR	Maximum Continuous Rating
MDO	Marine diesel oil
MGO	Marine gas oil
P_{AE}	Auxiliary Engine Power Output
P_{eff}	75% of the Installed Power for Each Usage Technology Used for The Propulsion of The Ship
P_{ME}	Engine Power Output
P_{PTI}	75% of Enterprise Power for Each Power Input System
P_{PTO}	Power of Shaft generator
Ro-Ro	Roll-on/roll-off
SFC	Specific fuel consumption
SFC_{AE}	Specific Fuel Consumption of P_{AE}
SFC_{ME}	Specific Fuel Consumption of P_{ME}
SHaPOLi	Shaft Power Limitation
V_{ref}	Ship Reference Speed
∇	Volumetric displacement

1. Introduction

The rise in global warming and the depletion of fossil fuels have accelerated research on energy efficiency and alternative energy systems worldwide.(Iqbal et al. 2024; Van Rheenen et al. 2024). The shipping industry has experienced this trend, which is a significant point since global trade vastly relies on marine vessels (Fang et al. 2020; Karatuğ et al. 2023). The main trends for the emission reduction strategies of the shipping industry have been categorised

CONTACT Onur Yuksel o.yuksel@ljmu.ac.uk Liverpool Logistics Offshore and Marine Research Institute (LOOM), Faculty of Engineering, Liverpool John Moores University, Byrom Street, Liverpool L3 3AF, UK; Zonguldak Bülent Ecevit University, Marine Engineering, Maritime Faculty, Hacı Eyüp Street, No:1 67300, Kdz. Ereğli/Zonguldak, Türkiye

This article has been corrected with minor changes. These changes do not impact the academic content of the article.

as technological, operational, and market-based approaches These include advancements in vessel design, optimised operations, and economic measures like carbon taxes and emissions trading schemes to promote sustainability (Huang et al. 2015).

International Maritime Organisation (IMO) has enforced the Energy Efficiency Existing Ship Index (EEXI) and Carbon Intensity Indicator (CII) to decrease the technical and operational carbon dioxide (CO_2) emission from commercial ships (Bayraktar and Yuksel 2023). The main goal of EEXI and EEDI is to inspect whether the existing and newly built ships meet energy efficiency reference values calculated based on ship types and capacity (Ivanova 2021). It shows the CO_2 emissions (in g) of a ship for every tonne of cargo handled across a one-nautical mile radius (ClassNK 2021b; Yuksel 2023). Similarly, CII focuses on the freight and total CO_2 emissions per navigated distance and sets a rating for the vessel as an energy efficiency indicator (ClassNK 2021a). The range of CII rating varies between A to E and marine vessels, having a D or below for three consecutive years must increase their energy efficiency performance (IMO 2023).

In light of these new and mandatory measures, enhancing energy efficiency on board has become a crucial concern for both existing and newly built vessels (Bayraktar et al. 2024; Yuksel 2025). Various applications have been proposed to improve energy efficiency and ensure compliance with regulations. The hull cleaning, energy-saving devices, alternative fuels, propulsion system enhancements, speed, and route optimisation can be listed as examples of these approaches (Bayraktar and Yuksel 2023; Göksu et al. 2024; IMO 2022c).

A prominent option for increased energy efficiency and decreased CO_2 emissions is a hybrid propulsion system (HPS). This approach is particularly advantageous for passenger and cruise ships, as it reduces fuel consumption, vibration, and noise levels. Additional benefits of the system include its quick response to load changes and enhanced reliability, which together result in a reduced requirement for spare parts (Inal et al. 2022). The system operates based on an integrated configuration comprising load-sharing generators, electric motors, and potentially batteries.

The electric motors have been used in the HPS offering significantly higher efficiency across various operational ranges. Power generation is facilitated by generator sets (gensets), with the flexibility to adjust the number of active generators based on demand. Additionally, batteries play a critical role in stabilising power output, balancing the load, and providing supplemental power when required (Hansen et al. 2001).

1.1. Literature review

Various studies have assessed the implementation of HPS and potential alternative marine fuels on different marine vessel types, considering economic, environmental, and energy efficiency aspects. Within the framework of these studies, Jeong et al. (2018) conducted a study utilising a decision-making framework to evaluate various propulsion options involving gensets, reckoning with economic, environmental, and safety concerns. The HPS was identified as environmentally friendly and more reliable for the reference vessel. Despite its high installation cost, the HPS proved to be cost-effective due to its enhanced energy efficiency and reduced maintenance requirements.

Zaccone et al. (2021) performed a genetic algorithm-based optimisation framework for an HPS. The algorithm identified the optimal HPS design and optimised load sharing based on the vessel's energy demands, achieving significant energy savings.

Zwierzewicz et al. (2022) developed two control strategies for permanent magnet synchronous motors utilised in HPS. Results demonstrated that these strategies have the potential to enhance the HPS's energy management performance.

Elkafas and Shouman (2022) investigated the emission reduction and energy efficiency increment potentials of an HPS on a passenger vessel and compared it with the conventional system. The CO_2 reduction was calculated at 10%, while the sulphur oxides (SO_x) and nitrous oxides (NO_x) were lowered at 88% and 21% respectively. The system additionally offered benefits by meeting the criteria set forth by the Energy Efficiency Design Index (EEDI).

Gospić et al. (2022) identified slow steaming and gas injection engines as effective short-term measures for decreasing fuel consumption in marine vessels. Their findings showed that slow steaming on container ships could lower CO_2 emissions by 22 kilotonnes annually. However, severe sea states increased resistance, necessitating higher power consumption for equivalent operations.

Farkas et al. (2022) highlighted that marine vessels built before 2016 often fail to meet increasingly stringent EEXI regulations. While slow steaming can reduce fuel consumption and support short-term EEXI compliance, it may lead to suboptimal engine loads, disrupting operations and reducing engine lifespan. The study argued that over-reliance on slow steaming delays the shift to alternative and renewable fuels, impeding the maritime sector's 2050 carbon neutrality objectives.

Farkas et al. (2023) noted that the advantages of implementing slow steaming differ notably subject to the liner ship routes and operating area where diverse sea conditions are encountered.

Zincir (2023) demonstrated that slow steaming is effective in meeting 2030 emission targets by reducing CO_2, CH_4, N_2O, and black carbon emissions that contribute to global warming. However, it increases operating costs, offsetting savings from reduced fuel consumption due to longer operating times.

Kalajdžić et al. (2023) emphasised that slow steaming strategies were not limited to ocean-going vessels but can also be implemented to enhance energy efficiency in inland shipping operations. However, energy efficiency gains were significantly altered by the nature and features of the rivers they voyage on.

Ammar et al. (2023) analysed the cost–benefit trade-offs and the EEXI decrease of HPS incorporating dual-fuel (DF) engines and fuel cells on liquefied natural gas (LNG) carriers. Their scenario-based analysis also included the impact of engine power limitation (EPL). The study found that the EEXI could be reduced by up to 17%. While the initial capital costs of HPS were lower compared to conventional LNG systems, operational costs were higher.

Acanfora et al. (2023) proposed an energy storage solution and a control method for HPS to optimise performance under heavy weather conditions. The model results demonstrated the proposed design's effectiveness in managing power demand fluctuations during operation.

Tuswan et al. (2023) highlighted LNG's potential as a marine fuel to meet IMO decarbonisation targets presenting considerable reductions in NO_x, SOx, and particulate matter (PM) emissions in an economically viable manner. Key factors for LNG-fuelled vessels included compliant engine and equipment placement, existing bunkering infrastructure, and adherence to crew requirements set by maritime authorities.

Pang et al. (2024) implemented an optimised control method for an LNG-powered HPS, incorporating battery degradation modelling. The proposed strategy achieved a 12.28% CO_2 reduction and cost savings of $305,286 over a decade, with a 12% loss in battery health.

Wang et al. (2024) explored a multi-faceted design optimisation approach for a small cruise ship with hybrid electric propulsion. The findings highlighted the advantages of the tri-optimal design method.

Hong et al. (2024) developed a control framework and optimisation method using dynamic programming to enhance the energy efficiency of an HPS. The presented approach achieved fuel savings of up to 9%.

The HPS usage on marine vessels is a contemporary topic, with most research emerging in the past five years. Economic factors, including initial investment, operating, and maintenance costs, have been analysed to address uncertainties in HPS adoption. From an environmental perspective, studies have highlighted the advantages of HPS in reducing CO_2, PM, SO_x, and NO_x, emissions, and meeting stringent maritime regulations. Studies have also explored algorithm development, control strategies, engine load optimisation, slow steaming, and alternative fuels to improve energy efficiency under EEDI and EEXI frameworks. Additionally, safety-focused papers have aimed to ensure smooth HPS operations.

1.2. Research gap and motivation

Despite extensive research on the energy efficiency, environmental, and economic benefits of HPS in marine vessels, few studies address its advantages in meeting IMO regulations. The novelty of this article is highlighted in the following points:

- Limited research focuses on ship compatibility with EEDI and EEXI. This study extends the analysis to include the CII and its rating.
- The compliance of HPS installation, alternative fuel use, and EPL application both separately and combined with these indices is evaluated, filling a gap in the literature.
- A novel contribution is the selection of optimal engine power output via EPL for HPS. This addresses the effectiveness of slow steaming measures, such as EPL, under various marine fuel scenarios, aligning with IMO's short-, medium-, and long-term goals.
- While existing research primarily targets passenger ships, cruise vessels, and cargo ships, there is a significant lack of studies focused on Ro-Ro (Roll-on/Roll-off) cargo ships. This study aims to fill that gap by analysing the noon report data of a Ro-Ro vessel.
- Unlike prior studies that examine alternative, renewable, or conventional fuels separately or in combination, this study uses dual-fuel engines capable of operating on LNG, methanol, and conventional fuels to assess compliance with energy efficiency indices.
- Resolution MEPC.364(79) implies that EEDI and EEXI formulas may not apply directly to ships with diesel-electric, turbine, or hybrid propulsion systems. This study's outcomes present valuable insights for maritime stakeholders and authorities for updating guidelines and formulas.

This research aims to analyse HPS utilisation in Ro-Ro cargo ships, incorporating both DF engines and EPL applications. Energy efficiency measures, including EEDI, EEXI, CII, and CII ratings, have been calculated and compared with reference values set by the IMO. Ship-specific design elements have been considered in the EEDI and EEXI calculations. The CII and CII ratings have been evaluated through 2026, following MEPC.338(76) and MEPC.354(78) guidelines. All indexes have been calculated for both conventional and DF engine applications. Alternative and conventional fuel usage within the hybrid propulsion system aims to minimise load fluctuations and ensure a smooth operation. LNG and methanol have been utilised in the selected DF engines, with LNG being the most used marine alternative fuel and methanol gaining popularity in new builds. Given the significant fuel savings from slow steaming, EPL application is essential for compliance with future regulations. This study aims to support sustainable development goals and enhance the body of literature on energy efficiency in maritime transport by presenting practical solutions.

2. Method

The section is divided into two subsections: 'System Description' and 'Mathematical Background." Figure 1 provides a detailed illustration of the stages of analysis.

The data collection from the reference Ro-Ro cargo ship initiates the analysis. The operational data has been gathered from the noon reports while the technical data has been found from the classification society records of the vessel. The data related to engines has been obtained from the manufacturers' datasheets. After the data collection and the decision on the engine types, the EEDI, EEXI, CII and the CII rating calculations have been performed for three different marine engines running on conventional and alternative marine fuels. The assessments related to results and the discussions about the potential precautions for the upcoming decarbonisation targets have been provided.

2.1. System Description

Ro-ro cargo shipping plays a substantial part in maritime transport as it is specifically designed to transport of high-value goods such as wheeled vehicles with built-in ramps on their bow or stern. The built-in ramps enable vehicles to load and unload independently, reducing the risks associated with cargo handling. This enhances personnel safety and minimises the time required for port operations (TransGlory 2021). Table 1 demonstrates the specifications of the investigated Ro-Ro Cargo ship working under a liner charter in the Mediterranean Sea.

The ship's build date is critical for determining the EEDI, as it affects the application of a reduction factor to the EEDI reference line ($EEDI_{Ref}$), which varies according to the ship type and capacity. Since the case study ship was built in 2019, it is evaluated within the scope of the EEDI Phase I restrictions, where a 5% reduction factor is applied as described in Resolution MEPC.328(76). In addition to the main ship particulars, the technical specifications of the main and auxiliary engines are essential for calculating the EEDI and EEXI. Table 2 provides details on the power outputs, specific fuel consumption (SFC), quantities, and transmission efficiencies of the main and auxiliary engines currently installed on the ship.

Conventional fuels are used in the marine engines, as detailed in Table 2, to meet both propulsion and hotel load requirements throughout the ship's operation. The fuel type is crucial for computing EEDI, EEXI, CII, and the CII rating, directly impacting compatibility with these indices essential for sustainable maritime transportation. Consequently, the lower calorific values (LCVs), carbon contents, and carbon factors (C_F) are provided in Table 3, based on referenced sources.

Only the technical and chemical properties of MDO and HFO fuels are used to assess the Ro-Ro Cargo Ship's compliance with energy efficiency indices. Conversely, HFO, LFO, LNG, and methanol fuels, along with their respective properties, are considered in the developed HPS scenarios. In addition to fuel types and properties, the ship's speed is a key factor, particularly in calculating technical energy efficiency indices. The reference ship speed is directly linked to its installed power, with the required power varying based on the vessel's total resistance at the desired speeds, which depend on the ship's function and type. Figure 2 illustrates the speed-power curve of the case study ship, which is used in the EEDI and EEXI calculation processes.

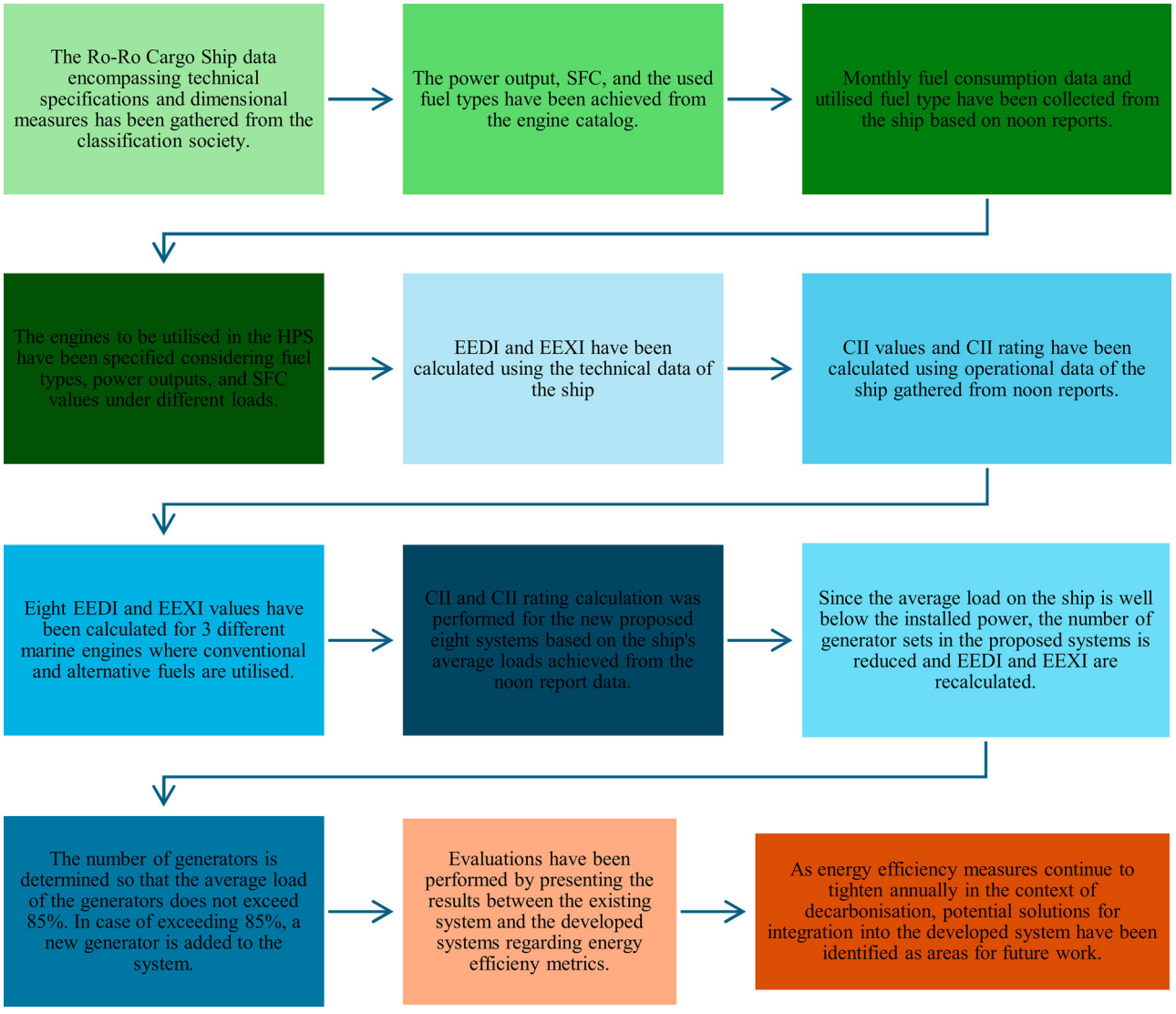

Figure 1. provides a detailed illustration of the stages of analysis.

Table 1. Ship particulars.

Specifications	Value/Classification	Units
Type of Ship	Ro-Ro Cargo Ship	-
Year of Build	2019	year
Length overall	237.4	m
Length between perpendiculars	232	m
Moulded Breadth	33	m
Draught (Summer Load Line)	7.1	m
Deadweight (DWT)	17183.45	t
Lightweight	17990.45	t
Gross Tonnage	60465	t
Ship Speed	20.97	kn
Displacement Volume	34302	m3

Table 2. The technical features of the main and auxiliary engines.

Technical Data	Value/Classification	Units
The main engine power @100% MCR	11800	kW
The number of main engines	2	Set
Fuel type	Diesel/Gas Oil	
SFC @ 75 % MCR	162.61	g/kWh
The auxiliary engine power @100% MCR	1980	kW
Fuel Type	Diesel/Gas Oil	
SFC at 50 % MCR	198	g/kWh
Alternator Efficiency	0.974	
The number of auxiliary engines	2	Set
The power output of the shaft generator	2350	kW
The number of shaft generator	2	Set

Based on the technical catalogue and measurements, the ship has been operated at a service speed of 20.97 kn with a power output of approximately 16,860 kW which is highlighted as the blue line in Figure 2. It also clearly reveals that small changes in service speed significantly reduce the required power installation of the ship.

This study proposes that the implementation of EPL will reduce power by approximately 30% to 40%, due to a decrease in the number of gensets used in the propulsion system, in line with energy efficiency measures. The red line in Figure 2 represents the reference speed/power output for the EPL application. The SFC values in Table 2 correspond to the lowest SFC at optimal load. As engine load decreases, SFC increases, particularly impacting the CII calculation, which is a key operational energy efficiency measure. To minimise the impact of load fluctuations on the indices, SFC rates and the load curve are developed based on noon reports, sea trials, engine tests (Bayraktar and Nuran 2022), and machinery catalogues. Figure 3 shows the SFC/Engine load curve and the corresponding formula.

Table 3. Details of marine fuels analysed in the study.

Fuel type	Reference	LCV (kJ/kg)	Carbon content	CF (t-CO2/t-Fuel)
MDO/MGO	(ISO 2017)	42,700	0.8744	3.206
HFO	(ISO 2017)	40,200	0.8493	3.114
Light Fuel Oil (LFO)	(ISO 2017)	41,200	0.8594	3.151
LNG	(IMO 2022b)	48,000	0.7500	2.750
Methanol	(IMO 2022b)	19,900	0.3750	1.375

The SFC versus engine load curve is modelled using a third-degree polynomial function, allowing for the calculation of SFC rates at various load levels. To explore scenarios utilising LNG, methanol, and conventional fuels, the implementation of new main engines or gensets is necessary. Consequently, three distinct marine engines have been selected to evaluate the impact of HPS on the Ro-Ro cargo ship across eight scenarios. The technical specifications of these selected marine engines are detailed in Table 4.

The Ro-Ro cargo ship, equipped with two main engines, has a total installed Maximum Continuous Rating (MCR) of 23,600 kW. This power output is considered in the selection of main engines for the developed scenarios. Within the framework of existing installed power, three different marine engines are chosen, considering both commercially available products and the number of generators on vessels utilising HPSs.

Engines I and II investigated the effect of both load distributions and alternative fuels under different operational conditions. The power outputs of Engine I, and II are 3360, and 2880 kW respectively and they are DF engines. In addition to conventional fuels, Engines I and II can use LNG and methanol.

Engine III operated with HFO and LFO fuels is only selected to assess load distributions under different operational conditions.

The number of units to be installed in the ship is seven, eight, and eight for main engines I, II, and III respectively.

These selections enable an in-depth analysis of HPSs utilising different engines on the ship, facilitating a comprehensive comparison of SFC rates, and emission profiles within the context of the energy efficiency measures. The simplified layout scheme of the HPS is illustrated in Figure 4.

Gensets, as prime movers, provide mechanical energy to the electrical generator, which produces electrical power. This power is transmitted to the main switchboard, a control unit through which all energy flows. Transformers are used to enhance the system's power-carrying capacity or to meet the voltage requirements of various

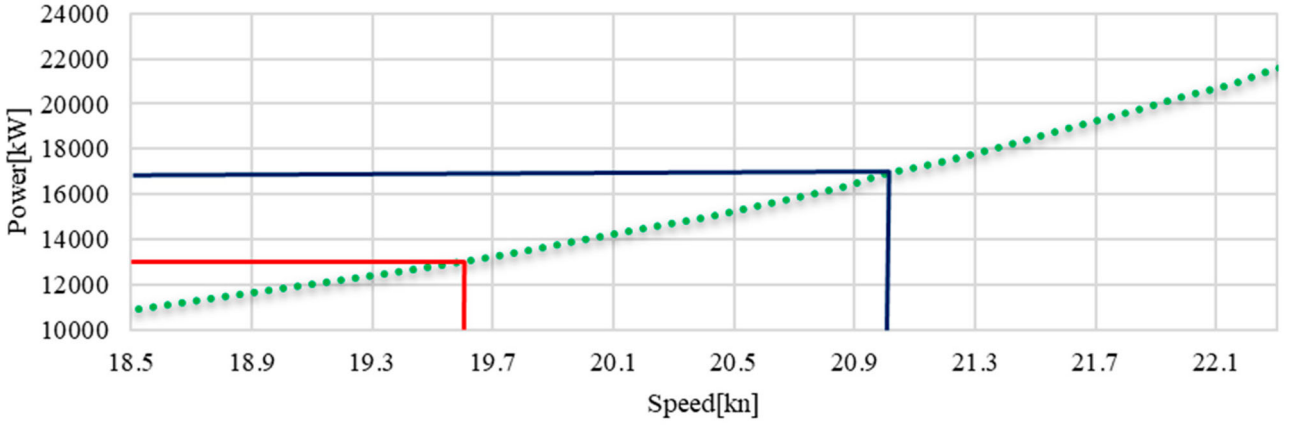

Figure 2. The speed-power curve of the Ro-Ro cargo ship.

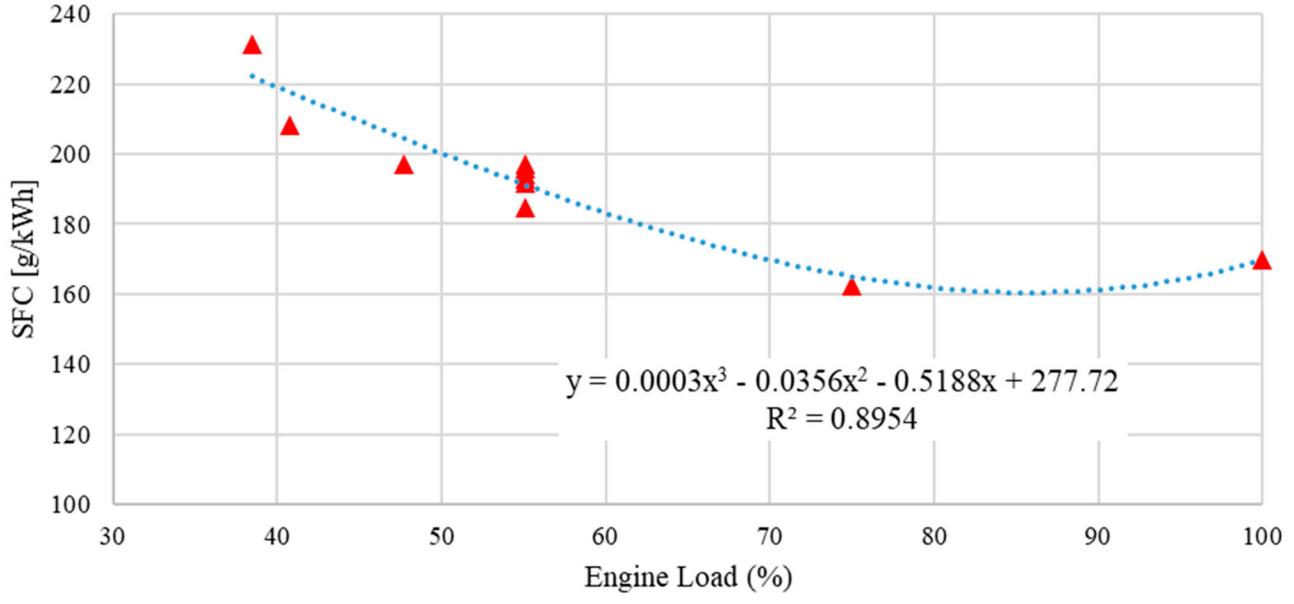

Figure 3. The curve fitting of engine load – SFC for the reference vessel.

Table 4. The specifications of engines and scenarios (Wärtsilä 2024).

Scenario	Engine	Cylinders	Engine Speed (rpm)	Engine Output (kW)	Fuel Type	SFC (g/kWh) or Specific Energy Consumption (kJ/kWh)			
					Engine Load	100%	85%	75%	50%
I	I	6	720	3360	HFO	185	185.5	185.8	196
II					LFO	186.9	184.7	184.9	192.7
III					Methanol	7800	7830	7890	8290
IV	II	6	720	2880	HFO	186.2	183.4	183.3	191.6
V					LFO	188.1	185.3	185.2	193.5
VI					LNG	7460	7620	7850	8590
VII	III	9	900	2925	HFO	191	190.6	193.9	203.2
VIII					LFO	192	191.5	194.9	204.2

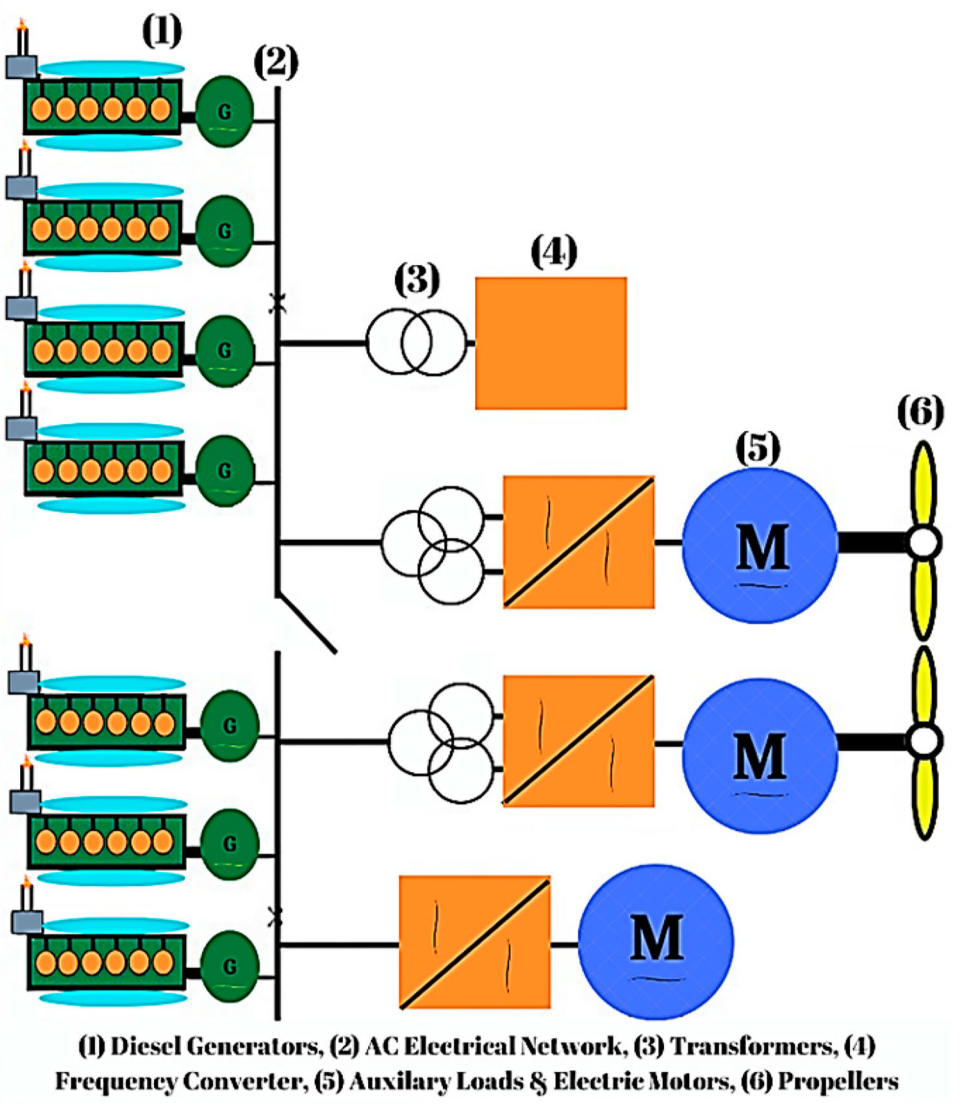

Figure 4. Simplified layout scheme of HPS.

equipment. The frequency converter is a key system component that converts alternating current (AC) to direct current (DC) or vice versa, enabling control of motor drives. Electric motors are powered by variable frequency drives fed by transformers. Additionally, energy storage devices can be integrated into the system for load balancing, energy backup, or to supply power to loads during periods of low demand (Geertsma et al. 2017; Morales Vásquez 2016).

2.2. Mathematical background

This section outlines the mathematical formulas employed in the analysis. Descriptions of the abbreviations used in the equations are available in the abbreviation list. Based on the technical catalogue and measurements, the ship operates at a service speed of 20.97 kn with a power output of approximately 16,860 kW. Small adjustments

in service speed can significantly affect the required power installation for the ship. Consequently, CII scenarios have been evaluated by varying the service speed by approximately 5%. The key parameters considered include main and auxiliary engine power, ship capacity, service speed, SFC, and the fuel carbon factor, which are essential for assessing compliance with the EEXI. Equation 1 calculates the EEXI and can also be utilised to compute the EEDI, applying different phase reduction factors as needed (IMO 2022b, 2022a; Bayraktar and Yuksel 2023).

$$
\begin{aligned}
&EEXI\ \&\ EEDI \\
&= \left(\prod_{j=1}^{n} f_j\right)\left(\sum_{i=1}^{nME} P_{ME(i)} x C_{FME(i)} x SFC_{ME(i)}\right) \\
&\quad + \left(P_{AE} x C_{FAE} x SFC_{AE^*}\right) \\
&\quad + \left(\left(\prod_{j=1}^{n} f_j x \sum_{i=1}^{nPTI} P_{PTI(i)} - \sum_{i=1}^{neff} f_{eff(i)} x P_{AEeff(i)}\right) C_{FAE} x SFC_{AE}\right) \\
&\quad - \left(\sum_{i=1}^{neff} f_{eff(i)} x P_{eff(i)} x C_{FME} x SFC_{ME^{**}}\right) \\
&\quad / \left(f_i x f_c x f_l x Capacity . f_w x V_{ref} x f_m\right)
\end{aligned}
\tag{1}
$$

The general formula consists of four basic parts. The first part focuses on carbon emissions of the main engines based on power output and SFC where:

- The engine or equipment type is designated by the subscript i, while the ship type is represented by the subscript j.
- P_{ME} is the main engine power (kW),
- SFC_{ME} is the specific fuel consumption of main engines (g/kWh),
- C_{FME} is the carbon emission factor of utilised marine fuels such as HFO, LNG, and MDO in main engines,
- f_j represents a correction factor that is based on specific design elements unique to the ship.

In the second part, emissions from auxiliary engines during power generation are addressed:

- P_{AE} refers the total nominal power of auxiliary engines (kW),
- SFC_{AE^*} is the specific fuel consumption of auxiliary engines (g/kWh).
- C_{FAE} is the carbon emission factor of marine fuels used in auxiliary engines.

The third part considers the impact of innovative systems within the framework of energy efficiency factors and emission reductions.

- P_{PTI} is a power provided by shaft motor,
- P_{PTO} is a power used by shaft generator,
- f_{eff} is the factor of each advanced energy efficiency technology,
- P_{eff} and is P_{AEeff} the advanced mechanical energy-efficient technology for the main and auxiliary engine respectively.

In the last part of the EEXI formulation:

- f_i is the capacity factor accounting for technical or regulatory limitations,
- f_c is the cubic capacity correction factor,
- f_l is the factor for general cargo ships fitted with cranes and cargo-related gear,
- f_w is a non-dimensional coefficient representing the speed reduction due to environmental conditions encompassing wave height/frequency, and wind speed,
- f_m is the factor for ice-classed ships capable of navigating challenging ice conditions with assistance from icebreakers when necessary.,
- V_{ref} is the ship speed, measured in nautical miles per hour (kn),
- *Capacity* is DWT for Ro-Ro cargo ships.

EEDI and EEXI are distinct metrics utilised to assess the energy efficiency of maritime vessels. The primary distinction between these indices lies in their application: EEDI pertains to newly constructed ships, whereas EEXI is relevant to existing vessels. Both indices share fundamental calculation methodologies, and their respective formulas exhibit considerable similarity (IMO 2022a).

The EEDIRef is tailored to each vessel based on its capacity, and various reduction factors corresponding to phases I, II, and III are applied depending on the year of construction and the type of ship. The EEXI is specifically designed for older vessels and incorporates a single reduction factor that varies according to the ship's capacity and type. For example, the reduction factor for cargo ships exceeding 2,000 DWT is typically set at 5%, while for cargo ships under 2,000 DWT, it ranges from 0% to 5% (IMO 2022a).

When calculating the EEXI for Ro-Ro cargo and passenger vessels, a correction factor (f_{jRoRo}) must be employed. Equation 2 demonstrates the formula for the f_{jRoRo} (IMO 2022b).

$$
f_{jRoRo} = \frac{1}{F_{n_L}^{\alpha} x \left(\frac{L_{pp}}{B_s}\right)^{\beta} x \left(\frac{B_s}{d_s}\right)^{\gamma} x \left(\frac{L_{pp}}{\nabla^{\frac{1}{3}}}\right)^{\delta}} \quad \text{If } f_{jRoRo} > 1 \ \textit{then}\ f_j = 1
\tag{2}
$$

where,

- $L_{pp}$is the length between perpendicular of the ship,
- B_s is the breadth of the ship,
- d_s is the summer load line draught,
- g is the gravitational acceleration.

The coefficients in the Equation 2 for a Ro-Ro cargo ship are as follows: α is 2, β is 0.5, γ is 0.75, and δ is 1. The Froude number (F_{n_L}) in Equation 2 can be computed by employing Equation 3 (IMO 2022b).

$$
F_{n_L} = \frac{0.5144 x V_{ref}}{\sqrt{L_{pp} x g}}
\tag{3}
$$

Capacity correction factor (f_i) accounting for technical/regulatory restrictions on capacity has been used in the EEDI and EEXI calculation phase on different ship types. Equation 4 is the formula for computing f_i.

$$
f_i = f_{i(ice\ class)} x f_{iCb}
\tag{4}
$$

For ship types other than tankers, general cargo or bulk carriers, the correction factor, f_{iCb} for improved ice-going capability is assumed to be 1. On the other hand, $f_{i(iceclass)}$ has differentiated to the ice class category. The formula for the ship in the ice class (IC) category is expressed in Equation 5 (IMO 2022b). IC category allows the ship to navigate in easy ice conditions in which ice thickness ranges from 0.15 to 0.30 meters (Sjöfartsverket 2024).

$$
f_i(IC) = 1.0041 + \frac{58.5}{\mathrm{DWT}}
\tag{5}
$$

The $\mathrm{EEDI_{Ref}}$ for the Ro-Ro vessel can be calculated by using Equation 6. The reduction factor for Ro-Ro cargo ships having a

capacity larger than 2,000 DWT has been determined regarding the built year (El Geneidy et al. 2018). Phase I covers the dates between 01 January 2015 and 31 December 2019 and a 5% reduction factor has been applied. Phase II requires a 20% reduction and includes the vessels built between 01 January 2020 and 31 December 2024. Finally, Phase III involves the ships after 01 January 2025 and a 30% reduction has been employed for these vessels' reference lines (ClassNk 2021c). Since our vessel was built in 2019, Phase I conditions have been valid, and a 5% reduction has been applied to the reference line in the calculations.

$$EEDI_{Ref} = 1405.15\ x\ DWT^{-0.498} \tag{6}$$

Ships require electrical energy, generated by auxiliary engines, to meet their hotel load and cargo operation needs. This power can be produced by gensets, shaft generators, waste heat recovery systems, and other onboard systems (Konur et al. 2023; Yuksel and Koseoglu 2023). Depending on the capacity of the shaft generator, it can significantly meet the electricity demands during navigation, often reducing or eliminating the reliance on gensets (Sarigiannidis et al. 2015).

The vessel is equipped with a shaft generator within its propulsion system, which is driven by the main engine and functions to generate electricity during operation. This system can meet a substantial proportion of the ship's electricity requirements. Conversely, vessels not equipped with shaft generators utilise conventional diesel generators to fulfil their electrical requirements. Therefore, the main engine and auxiliary engine effects for the EEDI and EEXI calculations should be updated in accordance with IMO MEPC.364(79) guidelines where $P_{PTO(i)}$ is 75% of the electrical power of each shaft generator $MCR_{PTO(i)}$ described in Equation 7.

There are two options to calculate the effect of shaft generators on the main and auxiliary engines within the framework of EEDI and EEXI calculations. The maximum allowable $P_{PTO(i)}$ reduction should not surpass $P_{AE}/0.75$. In this case, $\sum_{i=1}^{nME} P_{ME(i)}$ is defined in Equation 8 which is highlighted IMO (2022b) as Option I. For vessels with a total propulsion power of 10,000 kW or greater, P_{AE} is denotes the necessary auxiliary engine power allocated for propulsion and accommodation purposes. This value excludes the power consumed by other systems not directly involved in propulsion activities and is defined in Equation 9 (IMO 2022b).

$$P_{PTO(i)} = 0.75 x MCR_{PTO(i)} \tag{7}$$

$$\sum_{i=1}^{nME} P_{ME(i)} = 0.75x \sum MCR_{ME(i)} - 0.75x \sum P_{PTO(i)} \,\&\, \sum P_{PTO(i)} \leq \frac{P_{AE}}{0.75} \tag{8}$$

$$P_{AE} = \left(0.025x \left(\sum_{i=1}^{nME} MCR_{ME(i)} + \frac{\sum_{i=1}^{nPTI} P_{PTI(i)}}{0.75}\right)\right) + 250kW \tag{9}$$

Considering Equations 7, 8, and 9, the final formulation of EEXI and EEDI is addressed in Equation 10 (ClassNK 2021b; IMO 2022b). In addition, since the required electrical power is obtained from the shaft generator, the type of fuel used in the main engine and its carbon factor are used in the EEXI and EEDI calculation stage (IMO 2023).

$$\begin{aligned} EEXI = & \left(\prod_{j=1}^{n} \left(\frac{1}{\left(\frac{0.5144 x V_{ref}}{\sqrt{L_{pp} x g}}\right)^{\alpha} x \left(\frac{L_{pp}}{B_s}\right)^{\beta} x \left(\frac{B_s}{d_s}\right)^{\gamma} x \left(\frac{L_{pp}}{\nabla^{\frac{1}{3}}}\right)^{\delta}}\right)\right) \\ & \times x \left(\left(0.75x \sum MCR_{ME(i)} - 0.75x \sum P_{PTO(i)}\right) \right. \\ & \left. \times x C_{FME(i)} x\ SFC_{ME(i)}\right) \\ & + (((0.025 x MCR_{ME}) + 250kW) x (C_{FME(i)}\ x\ SFC_{ME(i)})) \\ & / \left(\left(\left(1.0041 + \frac{58.5}{DWT}\right) x f_{iCb}\right)\right. \\ & \left. \times x f_c x f_l x Capacity x f_w x V_{ref} x f_m\right) \end{aligned} \tag{10}$$

The steps to be followed in the EEXI and EEDI calculation phase are as follows:

- As f_j is a correction factor, the f_j value is computed regarding the vessel type in the first step using Equations 2 and 3 where L_{pp}, B_s, d_s are dimensional measures and they are obtained from classification society.
- MCR_{ME} and P_{PTO} are acquired from ship particulars. Moreover, SFC_{ME} are getting from from the records of engines certified according to the NOx Technical Code 2008.
- Based on the ship's noon reports and IMO MEPC.364(79) guidelines, fuel types and their C_{FME} are calculated.
- Since the ship does not have an PTI system, the PTI-related parts in the Equation 1 are not considered in the calculation.
- f_{eff}, P_{AEeff}, and P_{eff} are not considered because advanced energy efficiency technologies are not existed ship onboard.
- f_c, f_l, f_w, and f_m are calculated as 1 based on IMO MEPC.364(79) guidelines and f_i is calculated based on Equation 4 and 5. Ship capacity is used as DWT and f_{iCb} is acquired from IMO MEPC.364(79) guidelines.
- Within the IMO MEPC.364(79) guidelines framework, DWT is taken as the capacity measure.
- V_{ref} is the vessel reference speed and is measured in kn determined based on 75% of total installed propulsion power.

The calculation steps for Equation 10 are elucidated in a step-by-step manner using an example presented in Appendix. During the the required EEXI computation, the EEDI reference line value is used and a reduction factor (Y) at 5% according to the vessel type and capacity is applied as described in Equation 11 (IMO 2022a).

$$Attained\ EEXI \leq Required\ EEXI = \left(1 - \frac{Y}{100}\right) x\ EEDI\ reference\ line\ value \tag{11}$$

The attained CII calculated employing Equation 12, is the rate of the total CO2 mass (M) to the total transport work (W) carried out within a specific calendar year (IMO 2021a).

$$Attained\ CII = \frac{M}{W} = \frac{FC_j\ x\ C_{F_j}}{C\ x\ D_t} \tag{12}$$

Where j is the fuel type and FC_j is the fuel consumed in ship machinery systems, reported to the IMO DCS. The ship capacity is represented by C, and gross tonnage (GT) should be used as the

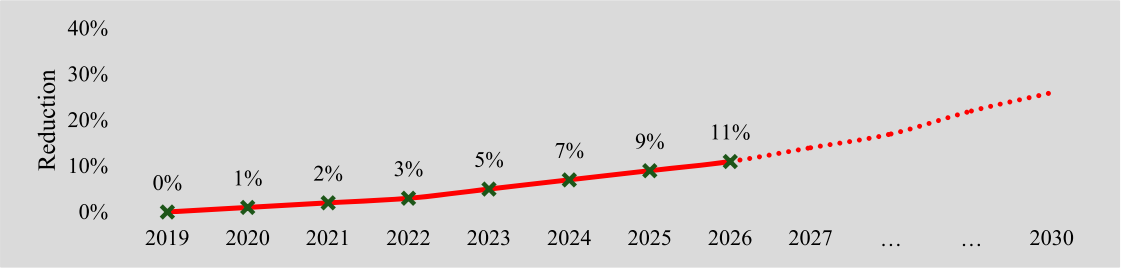

Figure 5. Reduction factor changes for CII reference lines.

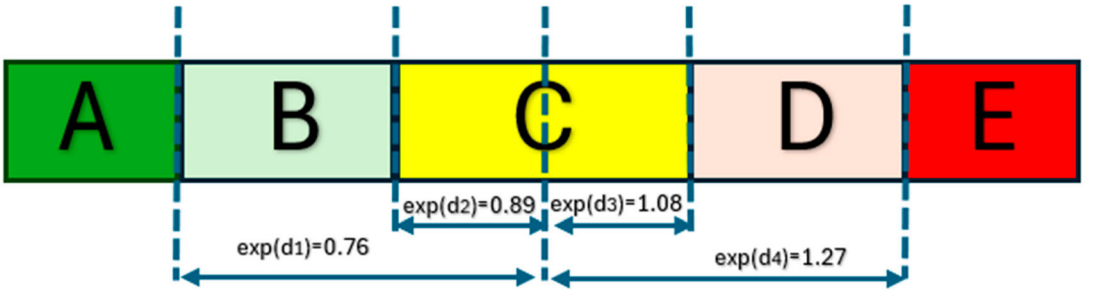

Figure 6. Exp (d_i) values and rating bands for the Ro-ro cargo ships (IMO 2022a).

capacity indicator for Ro-Ro vessels. It is recommended that GT be determined in accordance with the 1969 International Convention on Tonnage Measurement of Ships. The total travelled distance in nautical miles is represented by D_t (ClassNK 2021a). Equation 13 computes the reference CII (CII_{ref}) (IMO 2021a).

$$CII_{ref} = axCapacity^{-c} \tag{13}$$

The coefficients a and c have been 1967 and 0.485. The required CII is calculated by employing Equation 14 (ClassNK 2021a).

$$Required\ CII = (1 - Z/100)x\ CII_{ref} \tag{14}$$

The attained CII is identified as a reliable metric for assessing the operational carbon intensity of a vessel. The CII reference value, which represents the threshold for 2019 and is calculated for each ship type, is used for assessment purposes. A systematic reduction factor has been applied to this CII reference value, considering the vessel capacity and type. This systematic application of a continuously escalating reduction factor is crucial for ensuring sustainable maritime transport and eliminating greenhouse gases, with CO2 serving as the reference. Comparatively, the reduction rate for 2024 is set at 7%, increasing to 11% by 2026, irrespective of vessel types and capacities. By 2027 and in the years that follow, the reduction rate is anticipated to pose unprecedented challenges. This expectation is underpinned by the exponential growth of the reduction factor, as depicted in Figure 5 (Bayraktar and Yuksel 2023).

The reduction factors for the CII reference lines have risen and are expected to continue increasing in the coming years. For example, a tanker with a capacity of 100,000 DWT had a CII reference value of 4.67 in 2019. By 2024, this reference value is projected to decrease to 4.3431, indicating an applied reduction factor of 7%. Additionally, this reference value is expected to become even more stringent in subsequent years, highlighting the growing pressure on the shipping industry to improve its carbon efficiency.

Five grades, ranging from A to E, have been established to assess the ship's operational carbon intensity within the framework of energy efficiency boundaries. These boundaries are depicted in Figure 6 with the coefficient of boundaries for the Ro-Ro cargo ship. The expressions used to determine each boundary are expressed in Equation 15 (IMO 2021a).

$$\left.\begin{aligned} Superior\ Boundary &= exp\ (d_1)x\ Required\ CII \\ Lower\ Boundary &= exp\ (d_2)x\ Required\ CII \\ Upper\ Boundary &= exp\ (d_3)x\ Required\ CII \\ Inferior\ Boundary &= exp\ (d_4)x\ Required\ CII \end{aligned}\right\} \tag{15}$$

In 2019, boundaries were determined based on the CII distributions of each ship. The middle 30% of individual ships within the fleet are to be assigned a rating of C, upper 20% and further upper 15% of individuals are ranked D and E respectively. The remaining boundaries which are lower at 20% and further lower at 15% are also ranked B and A respectively (Bayraktar et al. 2023; Yuksel 2023).

The boundaries for evaluating carbon intensity are established based on the required CII calculated using reduction factors. This implies that operations performed by a ship in 2019 that achieved an 'A' rating in terms of CII may result in a lower rating, such as 'C' or below if the same operational profile is maintained in 2026. Consequently, as time progresses and ship types evolve, the boundaries and rating thresholds will also change. Maintaining A and B ratings will become increasingly challenging for vessels (Bayraktar and Yuksel 2023).

3. Findings and discussions

The coefficients for the reference Ro-Ro ship type utilised in the EEDI and EEXI calculations are derived from the formulas established in the mathematical modelling phase. The calculated coefficients, along with the remaining coefficients taken as one are presented in Table 5.

The main parameters required for EEDI and EEXI calculations, along with their respective values for the Ro-Ro ships, are presented in Table 6.

Since the ship was constructed in 2019, it meets the Phase I EEDI requirements. The EEDI Phase I reference value for the case study vessel aligns with the required EEXI value, as a 5% reduction factor is applied to the EEDI Phase 0 for Ro-ro vessels as outlined in IMO

Table 5. Coefficients of the case study ship for EEDI and EEXI calculation.

Parameters	Value	References
f_{jRoRo}	0.3264	IMO (2022b) and Equations 2–3
f_i	1.008	IMO (2022b) and Equations 4–5
f_c	1	IMO (2022b)
f_w	1	
f_l	1	
f_m	1	

Table 6. The main parameters of EEDI and EEXI calculations.

Parameters	Value	Unit	References
CO2 Emission	3,306,601.119	g/h	IMO (2022a) and Equation 1–10
Transport Work	363,219.6421	tnm/h	
EEDI & EEXI	9.10359	gCO2/tnm	IMO (2022b)
Required EEDI	10.3839	gCO2/tnm	IMO (2021b) and Equations 6 and 11
Required EEXI	10.3839	gCO2/tnm	

(2021b) (MEPC.328(76)). The threshold values for Phases 0, I, II, and III of the 17,183.5 DWT Ro-Ro cargo ship are illustrated in Figure 7.

For a Ro-Ro cargo ship with a 17,183.5 DWT capacity constructed between January 1, 2020, and December 31, 2024, the EEDI Phase II value is set at 8.74. From January 1, 2025, onwards, the Phase III value will decrease to 7.65. Figure 8 illustrates the compatibility of the proposed models for the Ro-Ro cargo ship with EEDI Phases II and III.

The EEDI values for scenarios I, II, IV, V, VII, and VIII, where conventional fuels such as HFO and LFO are used, range from 9.74 to 10.64. While all these values meet Phase 0 standards, none comply with Phases II or III. Scenarios I, II, IV, and V align with Phase I requirements. Among the conventional fuel scenarios, Scenario IV (using HFO) performs the best, while Scenario VIII (using LFO) performs the worst. For alternative fuels, the EEDI values are 9.48 for Scenario III (methanol) and 7.67 for Scenario IV (LNG). Although Scenario V approaches the Phase III limit, it only satisfies Phase II criteria, whereas Scenario III fails to exceed Phase I standards.

To reduce the attained EEDI and EEXI values and achieve compliance with Phases II and III limits using specified conventional and alternative fuels, either EPL or installed power must be adjusted within permissible boundaries. Figure 9 illustrates the impact of reducing installed power based on the optimal scenarios highlighted in Figure 8 for each conventional and alternative fuel. Considering the ship's average monthly engine loads, 5, 6, and 6 generator sets will suffice for engines 1, 2, and 3, respectively, under a 30%-40% EPL application.

These applications, which could disrupt the ship's operations during sudden load demands, must be implemented with precision. While scenarios V and IV, utilising LFO and HFO respectively, approach the Phase III threshold of 7.65, they fail to surpass it. Scenario VI, which was initially close to Phase III without power reduction, easily exceeds the threshold following power reduction measures. Similarly, Scenario III, previously meeting only Phase I requirements, now complies with EEDI Phase III due to power reduction applications. Table 7 details the ship's monthly CII values alongside the updated CII values derived from the proposed scenarios.

As indicated in the Figure 5, meeting the CII_{ref} value will become more challenging because, by 2026, a total 11% reduction factor will be applied on CII_{ref} values set for 2019. CII reference values and CII rating boundaries of the ship between 2023 and 2026 are expressed in Table 8 and Figure 10.

As shown in Figure 5, meeting the CII_{ref} value will become increasingly challenging due to applying an 11% reduction factor on the CII_{ref} values established for 2019 by 2026. The CII_{ref} values and CII rating boundaries for the ship from 2023 to 2026 are detailed in Table 8 and illustrated in Figure 10.

Superiorities and weaknesses of the existing system and each scenario applied in the ship have been listed:

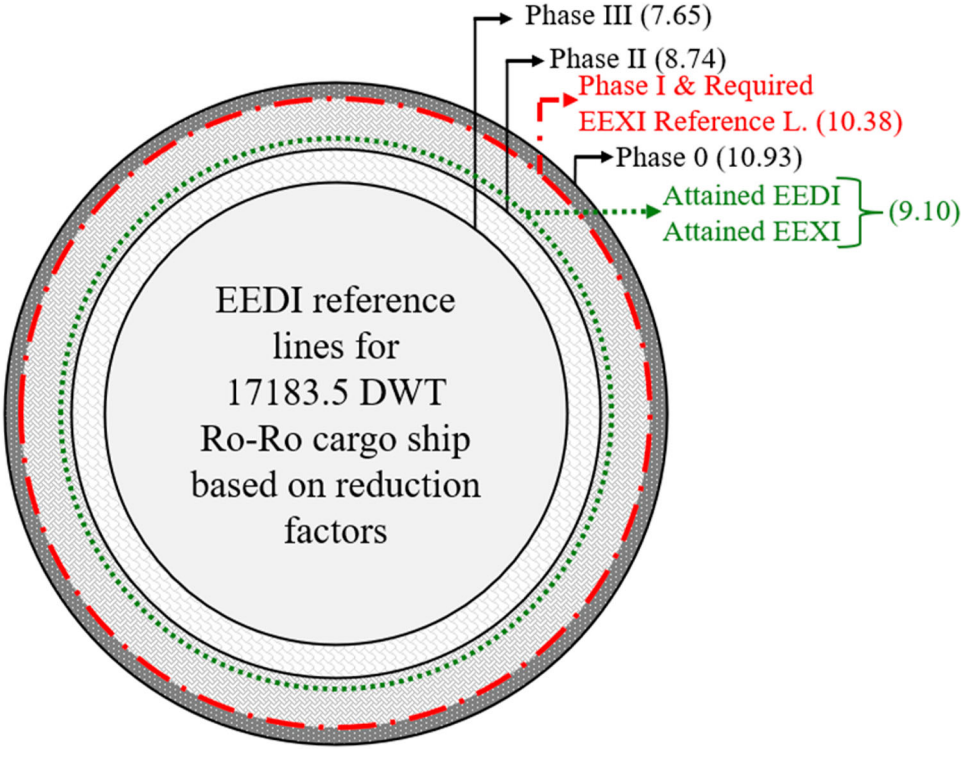

Figure 7. The EEDI Phases and EEXI reference value of a Ro-ro cargo ship with 17183.5 DWT capacity together with the attained EEDI and EEXI value of the ship.

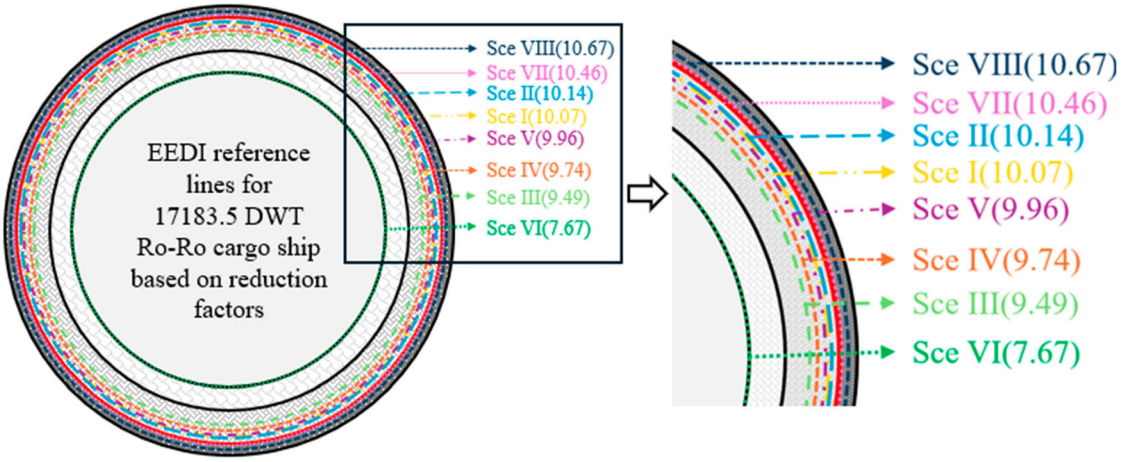

Figure 8. EEXI values of the scenarios.

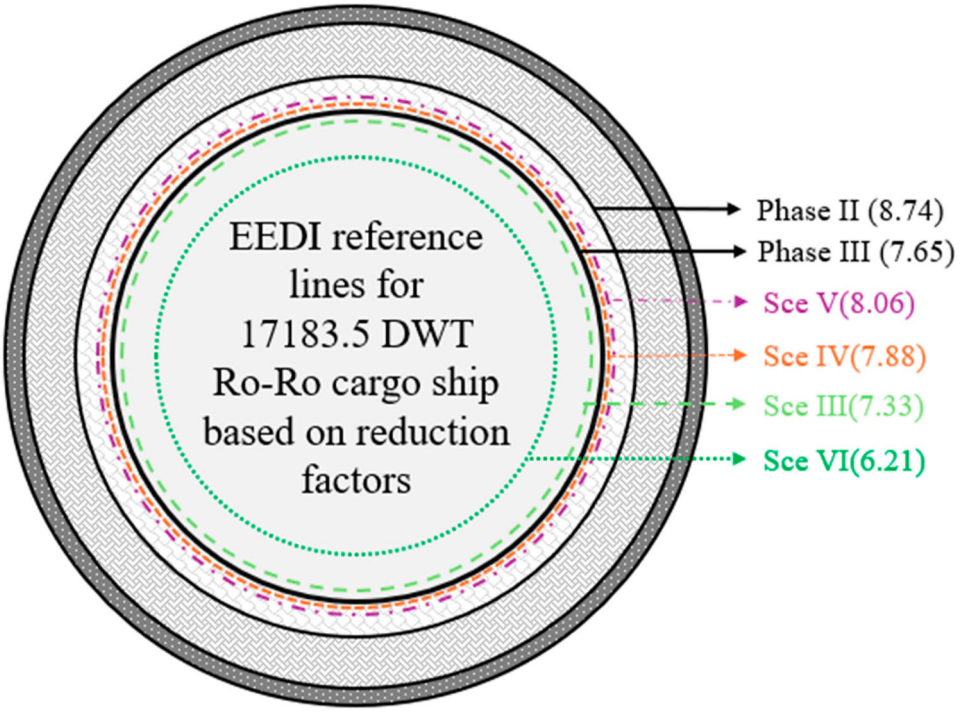

Figure 9. EEXI values for EPL-applied scenarios.

Table 7. Monthly CII values of scenarios.

Month	Existing	I	II	III	IV	V	VI	VII	VIII
1	6.5	5.34	5.36	5.05	5.2	5.31	4.13	5.45	5.51
2	6.71	6	6.03	5.66	5.9	6.03	4.57	6.13	6.2
3	7.16	6.76	6.81	6.35	6.69	6.83	5.26	7.02	7.1
4	7.18	7.14	7.19	6.74	7.06	7.22	5.64	7.47	7.56
5	7.11	6.9	6.93	6.51	6.75	6.9	5.26	7.05	7.13
6	6.86	6.29	6.33	5.92	6.22	6.36	4.96	6.58	6.66
7	7.13	6.9	6.93	6.51	6.75	6.89	5.26	7.05	7.14
8	7.07	6.53	6.58	6.15	6.45	6.59	5.14	6.82	6.9
9	7.32	6.81	6.86	6.41	6.73	6.88	5.36	7.1	7.18
10	7.09	6.55	6.6	6.17	6.47	6.61	5.15	6.84	6.92
11	7.11	6.6	6.65	6.21	6.52	6.66	5.17	6.88	6.96
12	7.42	6.97	7.02	6.56	6.89	7.04	5.46	7.24	7.32

Table 8. CII reference values and Boundaries of the ship based on the years.

Year	$\mathbf{CII_{ref}}$	Superior Boundary	Lower Boundary	Upper Boundary	Inferior Boundary
2023	8.96	6.81	7.98	9.68	11.38
2024	8.78	6.67	7.81	9.48	11.14
2025	8.59	6.53	7.64	9.27	10.90
2026	8.40	6.38	7.47	9.07	10.67

- Theship maintains CII ratings of A and B through 2026 with its existing propulsion system and voyage performance, and it avoids a C grade under all operational conditions even after 2026.
- Scenario I achieves an A-grade CII rating for some operations until 2026, with the rest at grade B, and no instances of a C grade are observed.
- Scenario II shows slightly lower CII values than Scenario I but maintains similar ratings throughout the specified period.
- Scenario III, using methanol as fuel, largely sustains an A-grade rating until 2026, with only a few months at grade B.

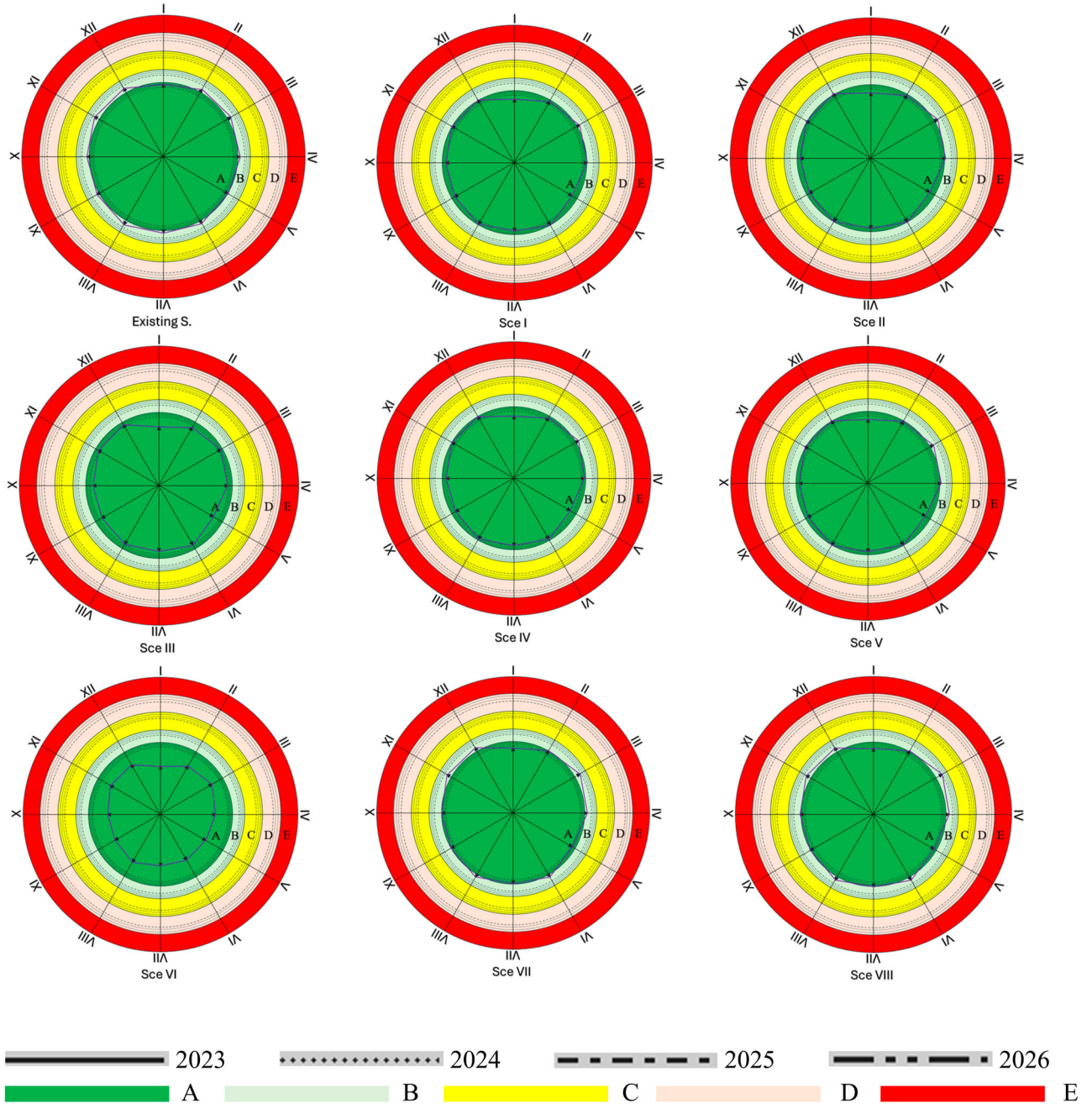

Figure 10. CII Ratings of scenarios.

- Scenarios IV, V, VII, and VIII, which utilise conventional fuels, generally result in B-grade ratings, similar to Scenarios I and II. However, Scenario VIII drops to a C grade in the fourth month of operation. Among these, Scenario IV achieves the best CII values but does not significantly outperform others in terms of ratings.
- Scenario VI, operated with LNG fuel, performs the best, consistently achieving an A-grade CII rating through 2026 and beyond.

Theapplicability challenges and limitations of the developed approach are highlighted in the context of utilising HPS and alternative marine fuels on a Ro-Ro cargo ship. These challenges stem from persistent technical, economic, and regulatory barriers associated with replacing conventional propulsion systems with HPS and adopting methanol or LNG as alternatives to conventional fuels.

- Methanol's energy density is lower than conventional and LNG fuels, necessitating larger fuel tanks, which reduce the ship's cargo capacity and potential earnings The presence of bunkering facilities is inevitable for the alternative fuel usage on ships (Svanberg et al. 2018).
- The availability of bunkering facilities is critical for adopting alternative fuels. While LNG bunkering facilities are gradually expanding, with 172 facilities worldwide (DNV 2024), methanol bunkering infrastructure remains limited, with only 120 facilities globally (Olufsen 2023). To promote alternative fuel usage globally, investments in bunkering infrastructure must increase.
- Fuel costs, accounting for 40–67% of marine vessel operating expenses, are pivotal in fuel selection (Ollila et al. 2024). LNG is currently the most expensive at $852/MT, compared to IFO380

and methanol at $473/MT and $433/MT, respectively (ShipandBunker 2024). Methanol's low energy density and LNG's high costs hinder widespread adoption, especially in regions with minimal environmental regulations.
- Reducing well-to-tank emissions is as crucial as minimising tank-to-wake emissions for sustainable maritime transport. Although green production methods for LNG and methanol reduce lifecycle emissions, they significantly increase costs (Olufsen 2023).
- Methanol's toxic and corrosive properties necessitate stringent safety measures and crew training to ensure safe and efficient operations (Deniz and Zincir 2016).
- While LNG engines offer advantages in reducing EEDI, EEXI, and CII values due to lower CO_2 emissions, they emit CH_4 having a global warming potential 27–30 times greater than CO_2 (IMO 2024). As indicated by EU ETS measures, this is likely to attract future regulatory scrutiny.
- HPS systems are more complex than conventional propulsion systems, leading to higher initial investment costs and increased operational complexity, which places additional responsibility on the crew.
- Alternative-fuel engines are available with power outputs comparable to conventional engines but lack the extensive diversity of power ratings seen in traditional systems (MAN 2024; Wärtsilä 2024).
- Integrating batteries into HPS systems can further reduce emissions. However, current battery technology lacks sufficient energy density for large-scale marine vessels. While increasing the number of batteries can meet energy demands, it adds weight and reduces onboard space. Recent advancements, such as lithium nickel manganese cobalt oxide (Li-NMC) pouch cells, show promise with energy densities of up to 450 Wh/kg (Liu 2023).

To facilitate the widespread adoption of HPS and alternative fuels in maritime transportation, it is essential to systematically eliminate existing shortcomings. Consequently, maritime stakeholders are intensifying their efforts to tackle these challenges.

- Technological advancements are driving down the costs of HPS installation and equipment, thereby attracting previously hesitant ship owners and operators to adopt these systems.
- Technological advancements are driving down the costs of HPS installation and equipment, thereby attracting previously hesitant ship owners and operators to adopt these systems.
- Significant progress has been made in reducing reliance on fossil fuels, transitioning to sustainable alternatives, and upgrading from conventional propulsion systems to advanced technologies. These developments are crucial for overcoming barriers to HPS and alternative marine fuels.
- Although alternative fuels currently have a higher unit price compared to conventional fuels, increasing reserves and innovations in production methods are lowering utilisation thresholds.
- The current bunkering facilities for alternative fuels, particularly LNG and methanol, are limited. However, many new facilities are being planned or discussed, which could enhance global accessibility.
- The IMO is advocating for the transition to more efficient systems by implementing energy efficiency regulations complicating conventional marine fuel usage.

In summary, these systems, along with various initiatives focused on enhancing energy efficiency and reducing carbon emissions, will be pivotal in advancing the IMO's short-, medium-, and long-term strategies.

4. Conclusion

A transition to alternative fuels and advanced propulsion systems on board is quite noteworthy to achieve sustainable maritime transportation and decarbonisation strategies. This study outlined the benefits derived from implementing an HPS using diverse marine engines on a Ro-Ro cargo vessel, emphasising advancements in fuel consumption savings and reductions in carbon emissions. The conclusions drawn from this study are as follows:

- Although transitioning from conventional propulsion systems to HPS using conventional fuels could lead to emissions reductions, these reductions did not exceed a certain threshold. This limitation arose because the carbon factors of HFO and LFO were higher than those of methanol and LNG.
- Despite its low carbon factor, the lower heating value of methanol presented a disadvantage, resulting in reduced energy output per unit volume compared to conventional marine fuels. Consequently, the low carbon factor of methanol contributed to emission reductions only when utilised in methanol-fuelled engines within HPS.
- LNG ranked between methanol and conventional fuels in terms of carbon factor but consistently outperformed diesel HPS scenarios due to its higher LCV.
- HPS integration minimised main engine load fluctuations by distributing loads across multiple engines, particularly in vessels that experience significant load variations during operations.
- HPS reduced fuel consumption while enhancing machinery lifespan and decreasing vibration and noise levels. Thus, HPS offered an innovative approach to sustainable maritime transportation.
- HPS powered by alternative fuels could be effectively implemented in various vessel types, such as tugboats and offshore supply vessels to adhere to energy efficiency standards These vessels often experience high load fluctuations and operate at low loads, making them suitable candidates for such technologies.

This study evaluated the advantages of HPS utilising traditional fuels, methanol, and LNG on Ro-Ro cargo ships. It addresses a significant research gap by comprehensively exploring the integration of HPS and alternative marine fuels concerning fuel consumption and carbon emissions while considering energy efficiency indices.

While these fuels and innovations in marine engines and HPS present substantial benefits for meeting EEDI, EEXI, and CII requirements, energy efficiency measures are becoming increasingly stringent. This trend suggests that reliance solely on these advancements may not suffice. Future research could provide valuable insights by investigating the use of ammonia or hydrogen in marine engines integrated with HPS. Although engines designed for direct ammonia and hydrogen use are still in early development, their adoption is essential for achieving carbon neutrality targets by 2050. Additionally, various after-treatment systems, such as carbon capture and storage, could serve as interim solutions until zero-emission fuels gain widespread acceptance by 2050.

Disclosure statement

No potential conflict of interest was reported by the author(s).

ORCID

Onur Yuksel http://orcid.org/0000-0002-5728-5866
Murat Pamik http://orcid.org/0000-0003-3268-1368

Murat Bayraktar http://orcid.org/0000-0001-7252-4776

References

Acanfora M, Balsamo F, Fantauzzi M, Lauria D, Proto D. 2023. Design of an electrical energy storage system for hybrid diesel electric ship propulsion aimed at load levelling in irregular wave conditions. Appl Energy. 350:121728–121739.

Ammar NR, Almas M, Nahas Q. 2023. Economic analysis and the EEXI reduction potential of parallel hybrid dual-fuel engine–fuel cell propulsion systems for LNG carriers. Pol Marit Res. 30(3):59–70.

Bayraktar M, Göksu B, Yüksel O. 2024. Matching of propulsion system components for a planing hull model. Ships Offsh Struct. 1–12. doi:10.1080/17445302.2024.2356949.

Bayraktar M, Nuran M. 2022. An assessment of electric motors from the point of marine propulsion systems. World Journal of Environmental Research. 12(1):43–49.

Bayraktar M, Yuksel O. 2023. A scenario-based assessment of the energy efficiency existing ship index (EEXI) and carbon intensity indicator (CII) regulations. Ocean Eng. 278:114295–114307.

Bayraktar M, Yuksel O, Pamik M. 2023. An evaluation of methanol engine utilization regarding economic and upcoming regulatory requirements for a container ship. Sustainable Production and Consumption. 39:345–356.

ClassNK. 2021a. Carbon intensity indicator. [accessed 2024 May 24]. https://www.classnk.or.jp/hp/pdf/activities/statutory/seemp/CII_en.pdf.

ClassNK. 2021b. Outlines of EEXI regulation. [accessed 2024 May 24]. https://www.classnk.or.jp/hp/pdf/activities/statutory/eexi/eexi_rev3e.pdf.

ClassNk. 2021c. Summary of the outcomes of MEPC 75. [accessed 2025 January 1]. https://www.classnk.or.jp/hp/pdf/tech_info/tech_img/T1228e.pdf.

Deniz C, Zincir B. 2016. Environmental and economical assessment of alternative marine fuels. J Cleaner Prod. 113:438–449.

DNV. 2024. Alternative Fuels Insight (AFI). [accessed 2025 January 1]. https://www.dnv.com/services/alternative-fuels-insights-afi–128171/.

El Geneidy R, Otto K, Ahtila P, Kujala P, Sillanpää K, Mäki-Jouppila T. 2018. Increasing energy efficiency in passenger ships by novel energy conservation measures. Journal of Marine Engineering & Technology. 17(2):85–98.

Elkafas AG, Shouman MR. 2022. A study of the performance of ship diesel-electric propulsion systems from an environmental, energy efficiency, and economic perspective. Mar Technol Soc J. 56(1):52–58.

Fang S, Wang Y, Gou B, Xu Y. 2020. Toward future green maritime transportation: An overview of seaport microgrids and all-electric ships. IEEE Trans Veh Technol. 69(1):207–219.

Farkas A, Degiuli N, Martić I, Grlj CG. 2022. Is slow steaming a viable option to meet the novel energy efficiency requirements for containerships? J Cleaner Prod. 374:133915.

Farkas A, Degiuli N, Martić I, Mikulić A. 2023. Benefits of slow steaming in realistic sailing conditions along different sailing routes. Ocean Eng. 275:114143.

Geertsma R, Vollbrandt J, Negenborn R, Visser K, Hopman H. 2017. A quantitative comparison of hybrid diesel-electric and gas-turbine-electric propulsion for future frigates. In: IEEE Electric Ship Technologies Symposium (ESTS); Arlington, VA, USA. pp. 451–458. doi:10.1109/ESTS.2017.8069321..

Göksu B, Bayraktar M, Yüksel O. 2024. The evaluation of propeller boss cap fins effects for different pitches and positions in open water conditions. Journal of Ship Production and Design. 40(02):102–111.

Gospić I, Martić I, Degiuli N, Farkas A. 2022. Energetic and ecological effects of the slow steaming application and gasification of container ships. Journal of Marine Science and Engineering. 10(5):703–710. doi:10.3390/jmse10050703.

Hansen JF, ådnanes AK, Fossen TI. 2001. Mathematical modelling of diesel-electric propulsion systems for marine vessels. Math Comput Model Dyn Syst. 7(3):323–355.

Hong SH, Kim DM, Kim SJ. 2024. Power control strategy optimization to improve energy efficiency of the hybrid electric propulsion ship. IEEE Access. 12:22534–22545.

Huang Z, Shi X, Wu J, Hu H, Zhao J. 2015. Optimal annual net income of a containership using CO2 reduction measures under a marine emissions trading scheme. Transportation Letters. 7(1):24–34.

IMO. 2021a. Guidelines on the Operational Carbon Intesnity Rating of Ships (CII Rating Guidelines, G4). [accessed 2024 May 25]. https://wwwcdn.imo.org/localresources/en/OurWork/Environment/Documents/Air%20pollution/MEPC.339(76).pdf.

IMO. 2021b. Amendments To The Annex Of The Protocol Of 1997 To Amend The International convention for the prevention of pollution from ships, 1973, as modified by the protocol of 1978 relating thereto. [accessed 2024 June 24]. https://wwwcdn.imo.org/localresources/en/KnowledgeCentre/IndexofIMOResolutions/MEPCDocuments/MEPC.328(76).pdf.

IMO. 2022a. 2022 guidelines on the method of calculation of the attained energy efficiency existing ship index (EEXI). [accessed 2024 June 24]. https://wwwcdn.imo.org/localresources/en/KnowledgeCentre/IndexofIMOResolutions/MEPCDocuments/MEPC.350(78).pdf.

IMO. 2022b. Resolution MEPC.364(79) - 2022 guidelines on the method of calculation of the attained energy efficiency design index (eedi) for new ships. [accessed 2024 June 20]. https://wwwcdn.imo.org/localresources/en/KnowledgeCentre/IndexofIMOResolutions/MEPCDocuments/MEPC.364%2879%29.pdf.

IMO. 2022c. Rules on ship carbon intensity and rating system enter into force. [accessed 2024 May 07]. https://www.imo.org/en/MediaCentre/PressBriefings/pages/CII-and-EEXI-entry-into-force.aspx.

IMO. 2023. 2023 IMO Strategy on Reduction of GHG Emissions from Ships. [accessed 2024 April 24]. https://www.imo.org/en/OurWork/Environment/Pages/2023-IMO-Strategy-on-Reduction-of-GHG-Emissions-from-Ships.aspx.

IMO. 2024. 2024 guidelines on life cycle GHG intensity of marine fuels (2024 LCA Guidelines). [accessed 2024 November 13]. https://wwwcdn.imo.org/localresources/en/KnowledgeCentre/IndexofIMOResolutions/MEPCDocuments/MEPC.391(81).pdf.

Inal OB, Charpentier J-F, Deniz C. 2022. Hybrid power and propulsion systems for ships: current status and future challenges. Renewable Sustainable Energy Rev. 156:111965–111980.

Iqbal R, Liu Y, Zeng Y, Zhang Q, Zeeshan M. 2024. Comparative study based on techno-economics analysis of different shipboard microgrid systems comprising PV/wind/fuel cell/battery/diesel generator with two battery technologies: A step toward green maritime transportation. Renewable Energy. 221:119670–119670.

ISO. 2017. SO 8217 2017 Fuel Standard for marine distillate fuels. [accessed 2024 June 20]. https://marine.wfscorp.com/sites/default/files/d7/documents/sites/default/files/ISO-8217-2017-Tables-1-and-2-1-1.pdf.

Ivanova G. 2021. Analysis of the specifics in calculating the index of existing Marine energy efficiency EEXI in force since 2023. In: 2021 13th Electrical Engineering Faculty Conference (BulEF); Varna, Bulgaria. p. 1–4. doi:10.1109/BulEF53491.2021.9690805.

Jeong B, Oguz E, Wang H, Zhou P. 2018. Multi-criteria decision-making for marine propulsion: hybrid, diesel electric and diesel mechanical systems from cost-environment-risk perspectives. Appl Energy. 230:1065–1081.

Kalajdžić M, Vasilev M, Momčilović N. 2023. Inland waterway cargo vessel energy efficiency in operation. Brodogradnja. 74(3):71–89.

Karatuğ Ç, Arslanoğlu Y, Soares CG. 2023. Review of maintenance strategies for ship machinery systems. Journal of Marine Engineering & Technology. 22(5):233–247.

Konur O, Yuksel O, Aykut Korkmaz S, Ozgur Colpan C, Saatcioglu OY, Koseoglu B. 2023. Operation-dependent exergetic sustainability assessment and environmental analysis on a large tanker ship utilizing organic rankine cycle system. Energy. 262:125477–125490.

Liu J. 2023. Progress and status of battery500 consortium phase II. [accessed 2025 January 1]. https://www1.eere.energy.gov/vehiclesandfuels/downloads/2023_AMR/bat317_liu_2023_o%20-%20jun%20liu.pdf.

MAN. 2024. CEAS engine calculations. [accessed 2024 17/09/2024]. https://www.man-es.com/marine/products/planning-tools-and-downloads/ceas-engine-calculations.

Morales Vásquez CA. 2016. Evaluation of medium speed diesel generator sets and energy storage technologies as alternatives for reducing fuel consumption and exhaust emissions in electric propulsion systems for PSVs. Ciencia y Tecnología de Buques. 9(18):49–62.

Ollila S, Merkel A, Börjesson M. 2024. Effect of fuel prices on sailing speeds in short-sea shipping. Appl Econ. 1–17. doi:10.1080/00036846.2024.2364106.

Olufsen C. 2023. A sustainable methanol ship fuel supply chain for the maritime industry: developing a framework through a systematic literature review exploring the technological, economic, and regulatory challenges for a sustainable methanol ship fuel supply chain (SMSFSC). University of South-East Norway.

Pang B, Liu S, Zhu H, Feng Y, Dong Z. 2024. Real-time optimal control of an LNG-fueled hybrid electric ship considering battery degradations. Energy. 296:131170–131182.

Sarigiannidis A, Kladas A, Chatzinikolaou E, Patsios C. 2015. High efficiency Shaft Generator drive system design for Ro-Ro trailer-passenger ship application. In: 2015 International Conference on Electrical Systems for Aircraft, Railway, Ship Propulsion and Road Vehicles (ESARS); Aachen, Germany. pp. 1–6. doi:10.1109/ESARS.2015.7101529.

ShipandBunker. 2024. World bunker prices. [accessed 2024 June 25]. https://shipandbunker.com/prices.

Sjöfartsverket. 2024. Old and new depths in the charts. [accessed 2024 June 24]. https://www.sjofartsverket.se/sv/tjanster/sjokortsprodukter/kopa-sjokort2/Gamla-och-nya-djup-i-sjokorten/.

Svanberg M, Ellis J, Lundgren J, Landälv I. 2018. Renewable methanol as a fuel for the shipping industry. Renewable Sustainable Energy Rev. 94:1217–1228.

TransGlory. 2021. What are RORO ships and their advantages. [accessed 2025 January 02]. https://www.transglory.com/en/roro-ships-maritime-freight-transportation-advantages/.
Tuswan T, Sari DP, Muttaqie T, Prabowo AR, Soetardjo M, Murwantono TTP, Utina R, Yuniati Y. 2023. Representative application of LNG-fuelled ships: a critical overview on potential ghg emission reductions and economic benefits. Brodogradnja. 74(1):63–83.
Van Rheenen ES, Padding JT, Slootweg JC, Visser K. 2024. Hydrogen carriers for zero-emission ship propulsion using PEM fuel cells: an evaluation. Journal of Marine Engineering & Technology. 23(3):166–183.
Wang Z, Chen L, Wang B. 2024. Tri-objective optimal design of a hybrid electric propulsion system for a polar mini-cruise ship. Ocean Eng. 300:117355–117367.
Wärtsilä. 2024. Online engine configurator - Find the right ship engine for you. [accessed 2024 April 29]. https://www.wartsila.com/marine/engine-configurator.
Yuksel O. 2023. A comprehensive feasibility analysis of dual-fuel engines and solid oxide fuel cells on a tanker ship considering environmental, economic, and regulation aspects. Sustainable Production and Consumption. 42:106–124.
Yuksel O. 2025. Modelling of a cargo oil pump turbine system to find the optimum pump operation capacities through the design of experiments approaches. Ships Offsh Struct. 20(3):384–396. doi:10.1080/17445302.2024.2336679.
Yuksel O, Koseoglu B. 2023. Numerical simulation of the hybrid ship power distribution system and an analysis of its emission reduction potential. Ships Offsh Struct. 18(1):78–94.
Zaccone R, Campora U, Martelli M. 2021. Optimisation of a diesel-electric ship propulsion and power generation system using a genetic algorithm. Journal of Marine Science and Engineering. 9:6.
Zincir B. 2023. Slow steaming application for short-sea shipping to comply with the CII regulation. Brodogradnja. 74(2):21–38.
Zwierzewicz Z, Tarnapowicz D, German-Galkin S, Jaskiewicz M. 2022. Optimal control of the diesel–electric propulsion in a ship with PMSM. Energies. 15:24.

Appendix

EEXI calculation example

Table A1. EEXI calculation steps for the case study vessel.

$f_{jRoRo} = \frac{1}{F_{n_L}^{\alpha} x \left(\frac{Lpp}{B_s}\right)^{\beta} x \left(\frac{B_s}{d_s}\right)^{\gamma} x \left(\frac{Lpp}{\nabla^{\frac{1}{3}}}\right)^{\delta}}\ \alpha = 2, \beta = 0.5, \gamma = 0.75, \delta = 1$	$f_{jRoRo} = \frac{1}{0.051^{\alpha} x \left(\frac{232}{33}\right)^{\beta} x \left(\frac{33}{7.1}\right)^{\gamma} x \left(\frac{232}{34302^{\frac{1}{3}}}\right)^{\delta}}$	f_{jRoRo} =0.3264
$F_{n_L} = \frac{0.5144 x V_{ref}}{\sqrt{L_{pp} x g}}$	$F_{n_L} = \frac{0.5144 x 20.97}{\sqrt{232 x 9.81}} = 0.051$	
$\left(0.75x \sum MCR_{ME(i)} - 0.75x \sum P_{PTO(i)}\right) x C_{FME(i)} x SFC_{ME(i)}$	(0.75x23600-840) = 16,860 16,860kWx3.206x162.61 g/kWh = 8,789,584.3 = 8,789,584.3xf_{jRoRo}	≅2,868,685g-CO_2/h
$((0.025 x MCR_{ME}) + 250kW) x (C_{FME(i)} x\ SFC_{ME(i)})$	0.025∗23,600+250 = 840kW 840kWx3.206∗162.61g/kWh = 437,915.2344	≅437,915g-CO_2/h
$\left(\left(\prod_{j=1}^{n} f_j x \sum_{i=1}^{nPTI} P_{PTI(i)} - \sum_{i=1}^{neff} f_{eff(i)} x P_{AEeff(i)}\right) C_{FAE} x SFC_{AE}\right)$	-	-
$\left(\sum_{i=1}^{neff} f_{eff(i)} x P_{eff(i)} x C_{FME} x SFC_{ME^{**}}\right)$	-	-
$f_i = f_{i(iceclass)} x f_{iCb}$	1x $x f_{iCb}$	f_i = 1.008
$f_i(IC) = 1.0041 + \frac{58.5}{\mathrm{DWT}}$	$f_i(IC) = 1.0041 + \frac{58.5}{17183.5} = 1.008$	
$f_c x f_i x Capacity x f_w x V_{ref} x f_m$	1x1x17183.5x1x20.97x1 = 363,219.64	t∗nm/h
EEXI & EEDI	= (2,868,685.884+ 437,915.2344)/ 363,219.6	≅ 9.10359 gCO_2/tnm